NeuroImage: Clinical 34 (2022) 102999

Contents lists available at ScienceDirect

NeuroImage: Clinical

journal homepage: www.elsevier.com/locate/ynicl

Tractography of supplementary motor area projections in progressive speech apraxia and aphasia

Adrian Valls Carbo [a,b], Robert I. Reid [c], Nirubol Tosakulwong [d], Stephen D. Weigand [d], Joseph R. Duffy [e], Heather M. Clark [e], Rene L. Utianski [e], Hugo Botha [e], Mary M. Machulda [f], Edythe A. Strand [e], Christopher G. Schwarz [a], Clifford R. Jack [a], Keith A. Josephs [e], Jennifer L. Whitwell [a,*]

[a] Department of Radiology, Mayo Clinic, Rochester, MN, United States
[b] Department of Neurology, Hospital Clinico San Carlos, Health Research Institute "San Carlos" (IdISCC), Universidad Complutense de Madrid, Madrid, Spain
[c] Department of Information Technology, Mayo Clinic, Rochester, MN, United States
[d] Department of Quantitative Health Sciences, Mayo Clinic, Rochester, MN, United States
[e] Department of Neurology, Mayo Clinic, Rochester, MN, United States
[f] Department of Psychiatry and Psychology, Mayo Clinic, Rochester, MN, United States

ARTICLE INFO

Keywords:
DTI
Tractography
Apraxia of speech
Agrammatism
Primary progressive aphasia
Frontal aslant tract
Supplementary motor area

ABSTRACT

Progressive apraxia of speech (AOS) is a motor speech disorder affecting the ability to produce phonetically or prosodically normal speech. Progressive AOS can present in isolation or co-occur with agrammatic aphasia and is associated with degeneration of the supplementary motor area. We aimed to assess breakdowns in structural connectivity from the supplementary motor area in patients with any combination of progressive AOS and/or agrammatic aphasia to determine which supplementary motor area tracts are specifically related to these clinical symptoms. Eighty-four patients with progressive AOS or progressive agrammatic aphasia were recruited by the Neurodegenerative Research Group and underwent neurological, speech/language, and neuropsychological testing, as well as 3 T diffusion magnetic resonance imaging. Of the 84 patients, 36 had apraxia of speech in isolation (primary progressive apraxia of speech, PPAOS), 40 had apraxia of speech and agrammatic aphasia (AOS-PAA), and eight had agrammatic aphasia in isolation (progressive agrammatic aphasia, PAA). Tractography was performed to identify 5 distinct tracts connecting to the supplementary motor area. Fractional anisotropy and mean diffusivity were assessed at 10 positions along the length of the tracts to construct tract profiles, and median profiles were calculated for each tract. In a case-control comparison, decreased fractional anisotropy and increased mean diffusivity were observed along the supplementary motor area commissural fibers in all three groups compared to controls. PPAOS also had abnormal diffusion in tracts from the supplementary motor area to the putamen, prefrontal cortex, Broca's area (frontal aslant tract) and motor cortex, with greatest abnormalities observed closest to the supplementary motor area. The AOS-PAA group showed abnormalities in the same set of tracts, but with greater involvement of the supplementary motor area to prefrontal tract compared to PPAOS. PAA showed abnormalities in the left prefrontal and frontal aslant tracts compared to both other groups, with PAA showing greatest abnormalities furthest from the supplementary motor area. Severity of AOS correlated with tract metrics in the supplementary motor area commissural and motor cortex tracts. Severity of aphasia correlated with the frontal aslant and prefrontal tracts. These findings provide insight into how AOS and agrammatism are differentially related to disrupted diffusivity, with progressive AOS associated with abnormalities close to the supplementary motor area, and the frontal aslant and prefrontal tracts being particularly associated with agrammatic aphasia.

* Corresponding author at: Mayo Clinic College of Medicine and Science, 200 1st St SW, Rochester, MN, United States.
E-mail address: Whitwell.jennifer@mayo.edu (J.L. Whitwell).

https://doi.org/10.1016/j.nicl.2022.102999
Received 3 November 2021; Received in revised form 11 March 2022; Accepted 28 March 2022
Available online 30 March 2022

1. Introduction

Apraxia of speech and agrammatic aphasia are two distinct symptoms but can co-occur and be progressive in nature in the context of a neurogenerative disease; both relate to degeneration of the frontal lobe. Apraxia of speech (AOS) affects the capacity to plan motor commands which are necessary to produce prosodically and phonetically normal speech (Duffy, 2006; Duffy, 2013). In contrast, agrammatic aphasia affects grammatical language production, resulting in grammatical simplification, the omission of function words, and difficulty with syntax and verbs (Tetzloff et al., 2018b; Thompson et al., 1997). Patients with neurodegenerative AOS can either present with isolated AOS, diagnosed as primary progressive apraxia of speech (PPAOS) (Josephs et al., 2012), or can have concurrent progressive agrammatic aphasia (AOS-PAA) (Josephs et al., 2013). Less commonly observed are patients who present with progressive agrammatic aphasia in the absence of AOS, where the term progressive agrammatic aphasia (PAA) has been utilized (Tetzloff et al., 2019). Patients with agrammatic aphasia, either with or without AOS, would also meet criteria for the non-fluent variant of primary progressive aphasia (nfvPPA) (Gorno-Tempini et al., 2011). Patients with PPAOS do not have aphasia and hence do not meet the core clinical criteria of early and predominant deficits in language required for a diagnosis of primary progressive aphasia (Mesulam, 1982, 2001). In PPAOS patients, previous neuroimaging studies have found bilateral supplementary motor area (SMA) and dorsolateral premotor cortex atrophy on structural imaging (Josephs et al., 2012; Utianski et al., 2018a) and hypometabolism on fluorodeoxyglucose positron emission tomography (FDG-PET) (Botha et al., 2015; Josephs et al., 2010; Josephs et al., 2013; Josephs et al., 2012). These regions are also involved in AOS-PAA, with additional involvement of the left inferior frontal gyrus (IFG) (i.e., Broca's area) (Josephs et al., 2013; Tetzloff et al., 2019). Although the SMA can become involved in PAA it is not the focus of degeneration, with PAA patients showing atrophy and hypometabolism of the prefrontal cortex and anterior temporal lobes (Tetzloff et al., 2019). Abnormal diffusivity has been observed in the body of the corpus callosum and premotor aspects of the superior longitudinal fasciculus in both PPAOS and AOS-PAA in diffusion tensor imaging (DTI) studies (Josephs et al., 2013; Josephs et al., 2012; Whitwell et al., 2013a), with involvement of more anterior frontal white matter tracts in PAA (Tetzloff et al., 2019). However, these studies were voxel-level whole brain analyses and hence did not target specific tracts.

Due to the association between specific symptoms and atrophy in remote but connected areas, some investigators have focused on the vulnerability of specific networks which may be associated with certain deficits (Catani et al., 2012a). Exploring this hypothesis, functional connectivity analysis has shown that AOS severity in PPAOS patients is correlated with connectivity between right SMA and the rest of the language network (Botha et al., 2018). Tractography, which delves into the structural properties of white matter to examine the integrity along tracts, has in recent years extensively explored correlations between specific subtypes of primary progressive aphasia and tract-specific degeneration. Degeneration of the frontal aslant tract (FAT), which connects the SMA and IFG, has been associated with a decline in verbal fluency, especially in nfvPPA (Catani et al., 2013). Other studies have confirmed that damage in the FAT and tracts connecting the SMA, left premotor cortex and striatum can be identified in nfvPPA (Mandelli et al., 2014). However, no previous studies have investigated tractography in PPAOS or assessed the unique contributions of AOS and agrammatic aphasia to connectivity from the SMA, including the FAT. Investigating cohorts of patients in whom AOS occurs in isolation, i.e., PPAOS, and patients with agrammatic aphasia without AOS, i.e., PAA, provides a unique opportunity to assess the relative contributions of these neurological symptoms.

Our aim was to utilize tractography to assess breakdowns in structural connectivity from the SMA in PPAOS in comparison to both AOS-PAA and PAA patients. This area was selected because of two main reasons: (1) atrophy of the SMA has been associated with AOS and is the primary imaging finding in PPAOS (Josephs et al., 2013; Josephs et al., 2012; Whitwell et al., 2013b) and (2) the SMA is involved in functions associated with movement, spatial and temporal processing (Kotz and Schwartze, 2011; Mita et al., 2009), and speech processing (Hertrich et al., 2016), which enforces the biological plausibility of (1). According to autoradiography techniques in primates (Luppino et al., 1993; Rizzolatti et al., 1996) and tractography and postmortem dissection in humans (Bozkurt et al., 2017; Bozkurt et al., 2016; Catani et al., 2012b; Leh et al., 2007; Vergani et al., 2014), the SMA is connected to the contralateral SMA (via callosal fibers), to the precentral gyrus, to the pars opercularis of the IFG (via FAT), to the middle frontal gyrus (Catani et al., 2012b) and to the striatum, particularly the putamen (Bozkurt et al., 2017; Catani et al., 2012b; Leh et al., 2007). We focused on assessing these five tracts in a PPAOS cohort and compared tract degeneration in PPAOS with tract degeneration in AOS-PAA and PAA cohorts, to determine which tracts are specifically related to progressive AOS and agrammatic aphasia. We also assessed direct correlations between tract integrity and severity of these clinical symptoms. We hypothesized that progressive AOS and agrammatic aphasia would be associated with different SMA tracts, with agrammatic aphasia being particularly associated with the FAT.

2. Materials and methods

2.1. Participants

Patients that presented with any combination of progressive AOS or PAA were recruited by the Neurodegenerative Research Group (NRG) at Mayo Clinic, Minnesota, USA, into two NIH-funded grants between July 1st, 2010 and July 31st, 2019. All patients underwent detailed neurological, speech and language, and neuropsychological evaluations, and an MRI session that included diffusion (dMRI) and high resolution T1 weighted scans. Patients with concurrent illnesses that could account for speech-language deficits, or meeting criteria for another neurodegenerative syndrome, including the semantic or logopenic variants of PPA (Botha et al., 2015; Gorno-Tempini et al., 2011), possible or probable progressive supranuclear palsy (Höglinger et al., 2017) or corticobasal syndrome (Armstrong et al., 2013) were excluded. The study cohort comprised 90 patients with available dMRI scans, of which six were excluded from the study due to poor quality dMRI acquisitions. Of the remaining 84 patients, 36 were diagnosed with PPAOS, 40 with AOS-PAA, and eight with PAA. Fifteen cognitively normal healthy control participants were also recruited by NRG during this time and underwent identical MRI acquisitions; two of these were subsequently excluded due to poor quality dMRI. This study was approved by the Mayo Clinic IRB, and all participants gave consent to participate in the research study.

2.2. Speech and language evaluations

The detailed speech and language battery has been previously described (Josephs et al., 2012). For this study, the primary measure of AOS severity was the Apraxia of Speech Rating Scale (ASRS) version 2.0 which measures the presence and prominence of a number of clinical features associated with AOS (Strand et al., 2014). The primary measures of aphasia severity were the Western Aphasia Battery-Revised Aphasia Quotient (WAB-AQ) (Kertesz, 2007) and the Token Test part V (De Renzi and Vignolo, 1962). The WAB-AQ serves as a global measure of aphasia severity that encompasses lexical content, fluency, repetition, naming, and language comprehension. The Token Test part V measures auditory comprehension of different sentence structures. The Northwestern Anagram Test (NAT) (Weintraub et al., 2009), a measure of grammatical production integrity, was also performed in 50% of patients. The speech and language evaluations were video recorded and diagnoses were rendered by consensus between two or three speech-language pathologists after reviewing the recorded examination (JRD,

HMC, RLU and EAS). Judgments regarding the presence of AOS were made based on all spoken language tasks of the WAB plus additional speech tasks that included vowel prolongation, speech alternating motion rates (e.g. rapid repetition of 'puhpuhpuh'), speech sequential motion rates (e.g. rapid repetition of 'puhtuhkuh'), word and sentence repetition tasks and a conversational speech sample. Agrammatism was judged to be present if function word omissions or syntactic errors were present during the WAB picture description task, in general conversation, or in the narrative writing subtest of the WAB, or if performance was below expected on the Token Test or NAT. The designation of agrammatism was made independent of the motor characteristics of speech. A patient was diagnosed with PPAOS if AOS was present and there was no unequivocal evidence of aphasia (Josephs et al., 2012). A patient was diagnosed with PAA if agrammatism was present and any evidence of AOS was no more than equivocal. A patient was diagnosed with AOS-PAA if both AOS and agrammatism were present.

2.3. Neurological and neuropsychological evaluations

The neurological examination included the Montreal Cognitive Assessment Battery (MoCA) (Nasreddine et al., 2005) to assess general cognitive function, the brief questionnaire version of the Neuropsychiatric Inventory (NPI-Q) (Kaufer et al., 2000) to assess abnormal behaviors and neuropsychiatric features, and the Movement Disorders Society Sponsored Revision of the Unified Parkinson's Disease Rating Scale part III (MDS-UPDRS III) (Goetz et al., 2008) to assess parkinsonism. The neuropsychological evaluations included the Auditory Verbal Learning Test (AVLT) (Rey, 1964) to assess verbal memory, the Trail Making Test B (Spreen and Strauss, 1998) and the Delis-Kaplan Executive Function System (DKEFS) (Delis et al., 2001) card sort test to assess executive function.

2.4. Image acquisition

All patients underwent a standardized MRI protocol on one of three 3 T GE scanners. The protocol included a T1 weighted (T1w) 3D magnetization prepared rapid acquisition gradient echo (MPRAGE) sequence (repetition/echo/inversion times = 2300/3/900 ms; flip angle 8°, 26-cm field of view; 256 × 256 in-plane sagittal matrix with a phase field of view of 0.94, slice thickness = 1.2 mm, in-plane resolution = 1 mm) and a single-shot echo-planar imaging diffusion sequence (repetition/echo times = 8000/58 or 11300/68 ms; in-plane matrix 128/128; field of view 35 cm; phase field of view 0.66; 41 diffusion encoding directions evenly spread over a b = 1000 s/mm^2 shell and five non-diffusion weighted images; 2.7 mm isotropic resolution). Parallel imaging with 2x phase encoding acceleration was used for the diffusion MRI (dMRI) acquisition.

2.5. Diffusion image processing

After denoising (Veraart et al., 2016) the diffusion images, head motion and eddy current distortion was corrected using FSL's eddy program (Andersson et al., 2017; Andersson et al., 2016; Andersson and Sotiropoulos, 2016). We corrected for Gibbs ringing as described in (Kellner et al., 2016) and then skull stripped the images (Reid et al., 2018). The Rician noise bias was then removed using the noise image from denoising and the procedure outlined in (Koay et al., 2009). Diffusion tensors were estimated using nonlinear least squares fitting and used to calculate Fractional Anisotropy (FA) and Mean Diffusivity (MD) images in dipy (Garyfallidis et al., 2014).

Inspired by (Bhushan et al., 2015) we synthesized a T1w-like image from the dMRI in order to improve the accuracy of the dMRI-to-T1w registration. Briefly, the average of the diffusion weighted volumes was mapped to match the T1w contrast using a monotonic function, and the approximation was refined by matching the grey and white matter contrasts using probabilistic segmentations constructed using SPM (T1w) (Ashburner and Friston, 2005; Schwarz et al., 2017) and the diffusion tensor eigenvalues. ANTs (Avants et al., 2014) was used to calculate a nonlinear warp between the synthetic and actual T1w images and apply that warp to register the diffusion data to the subject's T1w image. Whole brain tractograms were then made in dipy using particle filtering tractography (PFT)(Girard et al., 2014). The tracking was probabilistic, using the continuous map stopping criterion (Girard et al., 2014), constrained spherical deconvolution (Tournier et al., 2007) with a step length of 0.125 mm, and a maximum turn angle per step 23.4°. A seed was placed in each T1w white matter voxel (≈ 20 seeds per diffusion voxel), but PFT only retains tracks that make it from grey matter to grey matter while staying within white matter in between. The grey/white matter/cerebrospinal fluid probabilistic segmentations used by PFT were estimated from the subject's T1w using SPM12 (Ashburner and Friston, 2005) with Mayo Clinic Adult Lifespan template settings and priors (https://www.nitrc.org/projects/mcalt/).

2.6. Regions of interest definition

Regions of interest (ROIs) were determined by examining the MPRAGE images with fslview (https://fsl.fmrib.ox.ac.uk) and employing a modified version of the automated anatomical labelling (AAL) atlas (Tzourio-Mazoyer et al., 2002). All ROIs were defined as spheres with a radius corresponding to the size of the gyrus using AAL regional definitions as guidelines. The following five ROIs were manually placed in each case in both hemispheres: 1) SMA: we set a ROI with a 13.25 mm sphere on a sagittal slice with its center in the most medial portion of superior frontal gyrus. This ROI included part of the lateral part of superior frontal gyrus in most cases, but it did not reach the preSMA region. 2) Broca's area: a 6 mm radius sphere was delineated in the opercular part of the IFG. In the right hemisphere, the ROI was defined according to the same criteria. 3) Putamen: a 6 mm radius sphere was defined in the middle region of the putamen in each hemisphere. 4) Motor cortex: a single sphere of 10 mm radius was defined in the precentral gyrus, immediately superior to the intersection between the inferior frontal sulcus and precentral sulcus. 5) Middle frontal gyrus: a sphere of 12 mm radius was outlined in the most posterior part of middle frontal gyrus according to a previous article[24].

2.7. Tractography dissection

Virtual dissections were performed in TrackVis (Ruopeng Wang, Van J. Wedeen, TrackVis.org, Martinos Center for Biomedical Imaging, Massachusetts General Hospital). In order to exclude fibers from neighboring tracts we used a length threshold for each tract. To dissect the FAT the first ROI was located in the SMA and the second in Broca's area or its anatomical equivalent in the right hemisphere, and tracts longer than 100 mm were excluded. The U fibers from the SMA to the motor cortex were defined with the first ROI located in the SMA and the second in the motor cortex, with tracts longer than 95 mm excluded. The SMA-putaminal fibers were dissected with the first ROI located in the SMA and the second in the putamen, with a length threshold set between 90 and 125 mm, depending on the individual's anatomy. The commissural SMA fibers were dissected with the first ROI placed in the left SMA and the second in the right SMA, with a length threshold set between 90 and 125 mm. The SMA to middle prefrontal gyrus fibers were dissected with the first ROI located in SMA and the second in the middle frontal gyrus and a length threshold between 70 and 90 mm. Fig. 1 shows examples of each of the dissected tracts.

To compare FA and MD between participants at corresponding locations we constructed tract profiles (measures of FA and MD sampled along tracts) using fiber bundling functions in dipy (Garyfallidis et al., 2012; Garyfallidis et al., 2018) and the method described by Yeatman and colleagues (Yeatman et al., 2012). Tract profiles were introduced by (Gong et al., 2005) and, as one-dimensional structures, bridge the gap between performing statistical comparisons on three dimensional

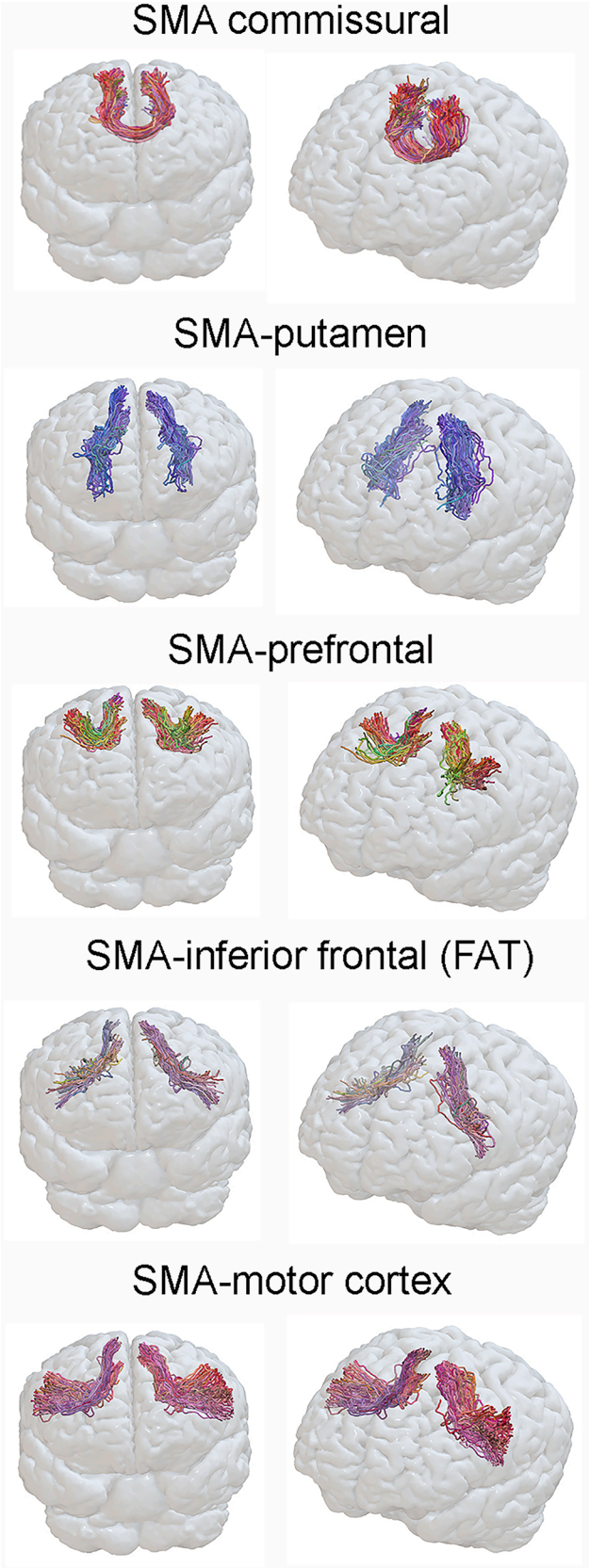

Fig. 1. Example dissections of each SMA tract. Each tract is shown on a three-dimensional rendering using Surf Ice software with two angled views.

images (voxel-based analysis (Smith et al., 2006)) and regions collapsed into points using atlas ROIs. Yeatman and colleagues (Yeatman et al., 2012) demonstrated (in a pediatric population) that tract profiles both outperform voxel-based analysis and retain useful position depended information that would be lost if only the mean or median FA and MD within a tract were used. After bundling a group of tracks into a tract, the tracks were resampled to each have the same number of points, set to the tract's upper length limit divided by the spatial resolution (2.0 mm). Each tract's "spine" was then defined as the centroid of its tracks, and weights w_{ij} were calculated for each point j of each track i to be proportional to the reciprocal of that point's Mahalonobis distance from the corresponding point on the bundle's spine. These weights were used to determine the average FA and MD along the tract:

$$\{FA, MD\}_{tract,j} = \sum_i w_{ij}\{FA, MD\}_{ij}$$

Examination of the resulting bundle profiles suggested that the spatial scale of the variation in FA and MD along the tracts was roughly 1 cm, suggesting that for statistical comparisons it would be appropriate to bin the profile FA and MD into 10 sections per tract. The binned values were calculated for each section k as.

$$\{FA, MD\}_{tract,k} = \sum_{j\in k} a_{tract,j}\{FA, MD\}_{tract,j} / \sum_{j\in k} a_{tract,j}$$

where $a_{tract,j}$ is the arc length of the tract's j^{th} piece.

2.8. Statistical analysis

The baseline participant characteristics were described using medians and inter-quartile ranges (IQRs) for continuous variables or counts and percentages for categorical variables. The AOS-PAA, PAA, PPAOS, and control (where applicable) groups were first compared using "global" tests in the form of analysis of variance or Fisher exact tests. Where the analysis of variance test was significant, Tukey's honest significant difference test was used to assess pairwise comparisons of the groups.

To analyze FA and MD profiles, linear mixed-effects models were fitted with the dMRI values as the response with a separate restricted cubic spline fit for each diagnosis group along with age at scan, scanner, and a random, subject-specific intercept to account for correlation among repeated measurements along the same tract within an individual. The spline treated locations 0–9 as numeric and specified outer knots at locations 1 and 8 and inner knots at 3.33 and 5.67. Using a restricted cubic spline with four knots allowed for a flexible functional form of the mean dMRI by tract location. This spline parameterization uses three degrees of freedom for each group and smooths, i.e. denoises, the fit and was preferred over the approach of treating each location as a separate level in a 10-level categorical variable. The latter would have required 9 degrees of freedom for each group, making for a model with many more parameters that would be much more susceptible to overfitting. Our model included MRI scanner as a fixed effect to account for any differences attributed to scanner.

Tract asymmetry was assessed as follows: left mean dMRI value – right mean dMRI value. We tested pairwise group differences in mean dMRI values and asymmetry scores across tracts using a joint Wald test with the null hypothesis being that mean values coincide across locations. We report pointwise 95% confidence intervals within group using parametric bootstrap simulations. Age at scan and scanner were included as covariates and results were corrected for multiple comparisons using the false discovery rate correction.

Partial spearman correlations were used to assess the relationship between median dMRI tract values and severity of AOS (measured using the ASRS) and agrammatic aphasia (measured using the Token Test), adjusted for age at scan and scanner.

All analyzes were performed in R version 3.6.3 using the lme4 and

arm packages.

3. Results

3.1. Demographic and cognitive data

Demographic and clinical data of all participants are summarized in Table 1. There were no significant differences among the disease groups for sex, education and apolipoprotein E (*APOE)* status. The PAA patients had a shorter disease duration at the time of the scan compared to the PPAOS patients.

The disease groups exhibited the expected speech and language deficits. The PPAOS patients showed preserved language abilities on the WAB, NAT and Token Test, with abnormal motor speech as shown on the ASRS; the AOS-PAA patients showed deficits in both motor speech and language testing; and the PAA patients showed normal scores on tests of motor speech, with deficits in language testing. On neuropsychological testing, AOS-PAA showed worse performance on the DKEFS card sort test compared to PPAOS, and PAA showed worse performance on AVLT delayed recall compared to both PPAOS and AOS-PAA.

Table 1
Demographic and clinical findings in the patient groups. Data shown as median (inter-quartile range) or n (%). APOE = apolipoprotein E; ASRS = Apraxia of Speech Rating Scale; AVLT = Auditory Verbal Learning Test; DKEFS = Delis-Kaplan Executive Function System; MDS-UPDRS III = Movement Disorders Society Sponsored Revision of the Unified Parkinson's Disease Rating Scale; MOANS = Mayo Older Americans Normative Studies; MoCA = Montreal Cognitive Assessment Battery; SUVR = standard uptake value ratio. Group-wise comparisons for continuous variables are from Analysis of Variance, followed by Tukey Honest Significant Differences. For categorical variables are from Fisher's Exact Test.

	AOS-PAA (n = 40)	PPAOS (n = 36)	PAA (n = 8)	Control (n = 13)	p value
Female, n (%)	19 (48%)	21 (58%)	5 (62%)	9 (69%)	NS
Age at MRI, years	70 (64, 74)	71 (62, 78)	69 (63, 75)	58 (56, 60)	0.002*
Disease duration, years	3.2 (2.5, 4.2)	3.8 (2.8, 5.3)	2.1 (2.0, 2.6)	NA	0.045†
Education, years	15 (12, 16)	16 (14, 18)	14 (12, 16)	14 (14, 16)	NS
APOE e4 carrier, n (%)	8 (20%)	7 (20%)	1 (12%)	NA	NS
Global Aβ SUVR	1.41 (1.30, 1.75)	1.35 (1.31, 1.44)	1.37 (1.32, 1.46)	1.35 (1.32, 1.41)	NS
ASRS total	20 (12, 27)	15 (12, 20)	4 (1, 5)	NA	<0.001‡
WAB aphasia quotient	86 (82, 93)	98 (96, 99)	87 (82, 90)	NA	<0.001§
WAB fluency	6 (5, 9)	10 (9, 10)	6 (6, 7)	NA	<0.001§
Token test	17 (12, 19)	20 (19, 21)	16 (13, 18)	NA	<0.001§
Northwestern Anagram Test	8 (6, 9)	10 (9, 10)	5 (4, 7)	NA	<0.001§
MoCA	24 (21, 25)	28 (26, 29)	24 (23, 24)	25 (24, 27)	<0.001§
MDS-UPDRS III	14 (6, 21)	12 (5, 18)	6 (3, 9)	NA	0.04#
AVLT Delayed Recall MOANS	9 (8, 11)	11 (10, 13)	6 (4, 8)	NA	<0.001§
Trail Making Test A MOANS	7 (5, 10)	8 (7, 11)	7 (6, 10)	NA	NS
Trail Making Test B MOANS	7 (4, 9)	9 (7, 10)	8 (6, 10)	NA	NS
DKEFS Card Sort MOANS	8 (6, 10)	12 (10, 14)	7 (7, 9)	NA	<0.001¶

* Control is statistically different from AOS-PAA and PPAOS.
† PPAOS is statistically different from PAA.
‡ PAA is statistically different from AOS-PAA and PPAOS.
§ PPAOS is statistically different from AOS-PAA and PAA.
‖ All groups are statistically different from each other.
¶ PPAOS is statistically different from AOS-PAA.
# PAA is statistically different from AOS-PAA.

3.2. Tractography findings

The profiles of FA and MD along the tracts are shown in Figs. 2 and 3. Differences in median number of streamlines, median FA and median MD along the tracts are summarized in Table 2.

3.2.1. PPAOS and AOS-PAA

The PPAOS and AOS-PAA groups both showed strikingly different profiles of FA and MD in the SMA commissural tract compared to controls, with higher MD and lower FA values compared to controls, and with greatest abnormalities observed in the middle of the tract (Figs. 2 and 3). Both groups also showed significantly abnormal profiles of both FA and MD along all other tracts from the SMA compared to controls, with the only exception being FA in the right FAT and the right SMA-motor tract. The profiles showed that the greatest abnormalities were observed closest to the SMA in most tracts, particularly for the MD profiles, except for the SMA-motor tracts where abnormalities were observed along the tract, and the commissural fibers where the greatest abnormalities were observed in the middle of the tract. The AOS-PAA group showed a different profile of MD in the left and right SMA-prefrontal tracts compared to PPAOS, with higher MD observed in AOS-PAA across the tract.

Similar findings were observed when assessing median FA and MD across the entire tracts (Table 2). The most significant differences observed for PPAOS compared to controls were in the left SMA-motor tract for FA ($p < 0.01$) and SMA commissural fibers for MD ($p < 0.05$). The most significant differences observed for AOS-PAA compared to controls were in the left and right SMA-prefrontal tracts ($p < 0.01$) and left SMA-motor tract ($p < 0.01$) for FA, and in the left SMA-motor tract ($p < 0.001$), as well as left SMA-prefrontal, left FAT, left SMA-putamen and commissural tracts (all $p < 0.01$) for MD.

3.2.2. Progressive agrammatic aphasia (PAA)

The PAA group showed significantly different profiles of MD and FA compared to controls in the bilateral SMA-prefrontal tract and the left FAT, with greatest abnormalities observed furthest from the SMA, i.e., closest to the prefrontal cortex for the SMA-prefrontal tract and closest to the IFG for the FAT (Figs. 2 and 3). The PAA group also showed an abnormal MD profile for the SMA commissural fibers compared to controls. No abnormalities were observed for the SMA-putamen and SMA-motor tracts.

PAA showed different FA and MD profiles from both PPAOS and AOS-PAA in the right SMA-putamen tract, with PPAOS and AOS-PAA showing greater abnormalities closest to the SMA and PAA showing greater abnormalities furthest from the SMA. Differences in MD were also observed for the SMA-prefrontal tracts, with PPAOS and AOS-PAA showing greater abnormalities compared to PAA, particularly close to the SMA. Differences in MD were observed in the left FAT, with PAA showing greater abnormalities than both PPAOS and AOS-PAA, particularly in the part of the tract closest to the inferior frontal gyrus. AOS-PAA showed more abnormal MD across the left SMA-motor tract compared to PAA.

Differences in median FA and MD between PAA and controls were observed for the left SMA-prefrontal tract ($p < 0.01$ for FA), left FAT ($p < 0.05$) and right SMA-prefrontal tract for FA ($p < 0.05$) (Table 2). No differences were observed across the three disease groups in any median tract metric.

3.2.3. Tract asymmetry

There was no difference in the degree of asymmetry in FA across groups for any tract. However, the degree of asymmetry in the SMA-

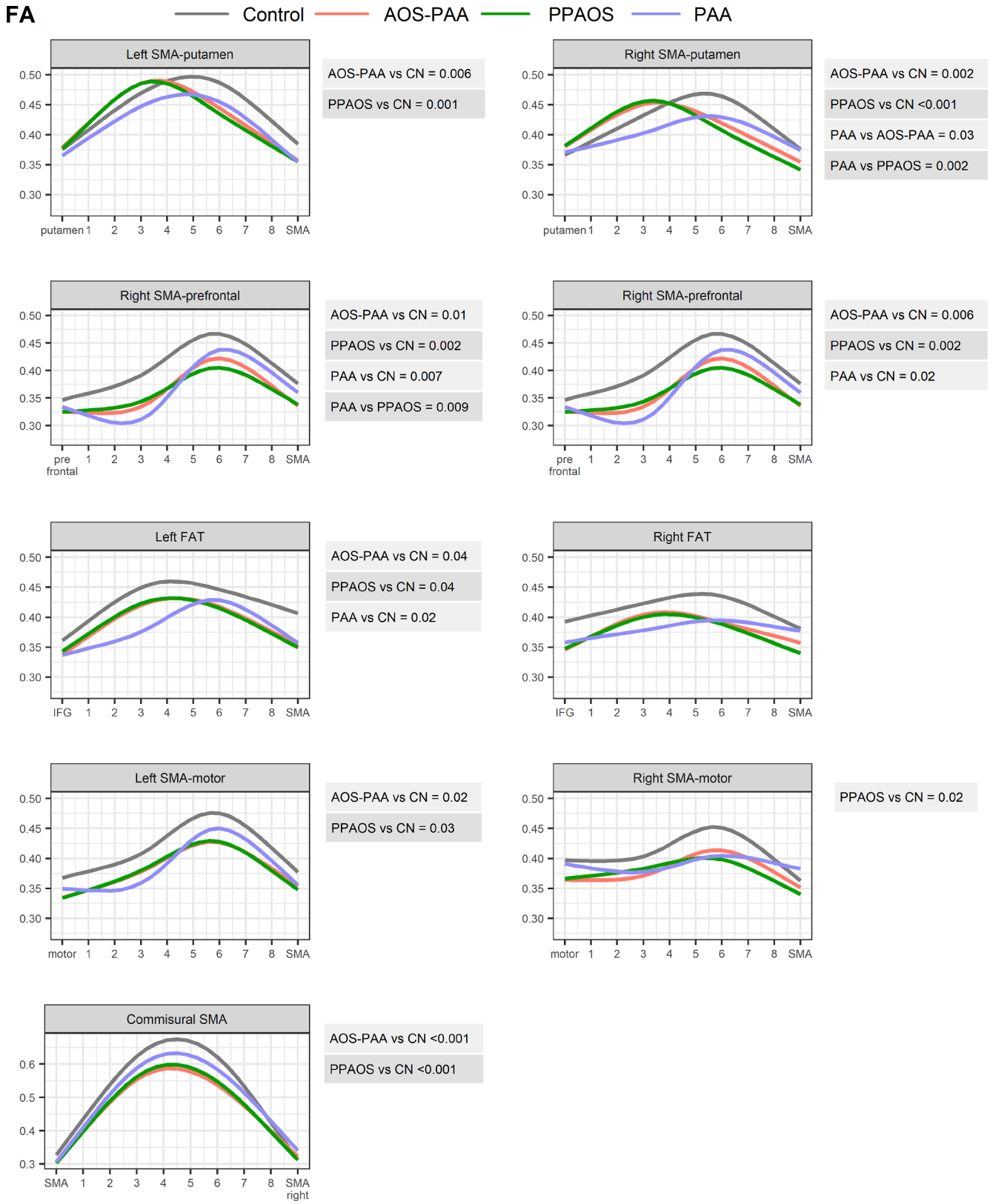

Fig. 2. Comparison of FA profiles between PPAOS, AOS-PAA, PAA and controls across tracts. Estimates from linear mixed models with restricted cubic spline fits are shown color coded for each diagnosis group for each SMA tract. P-values from a joint Wald test are shown for all significant group comparisons to the right of each plot. In the plots the first location represents the end of the tract furthest from the SMA.

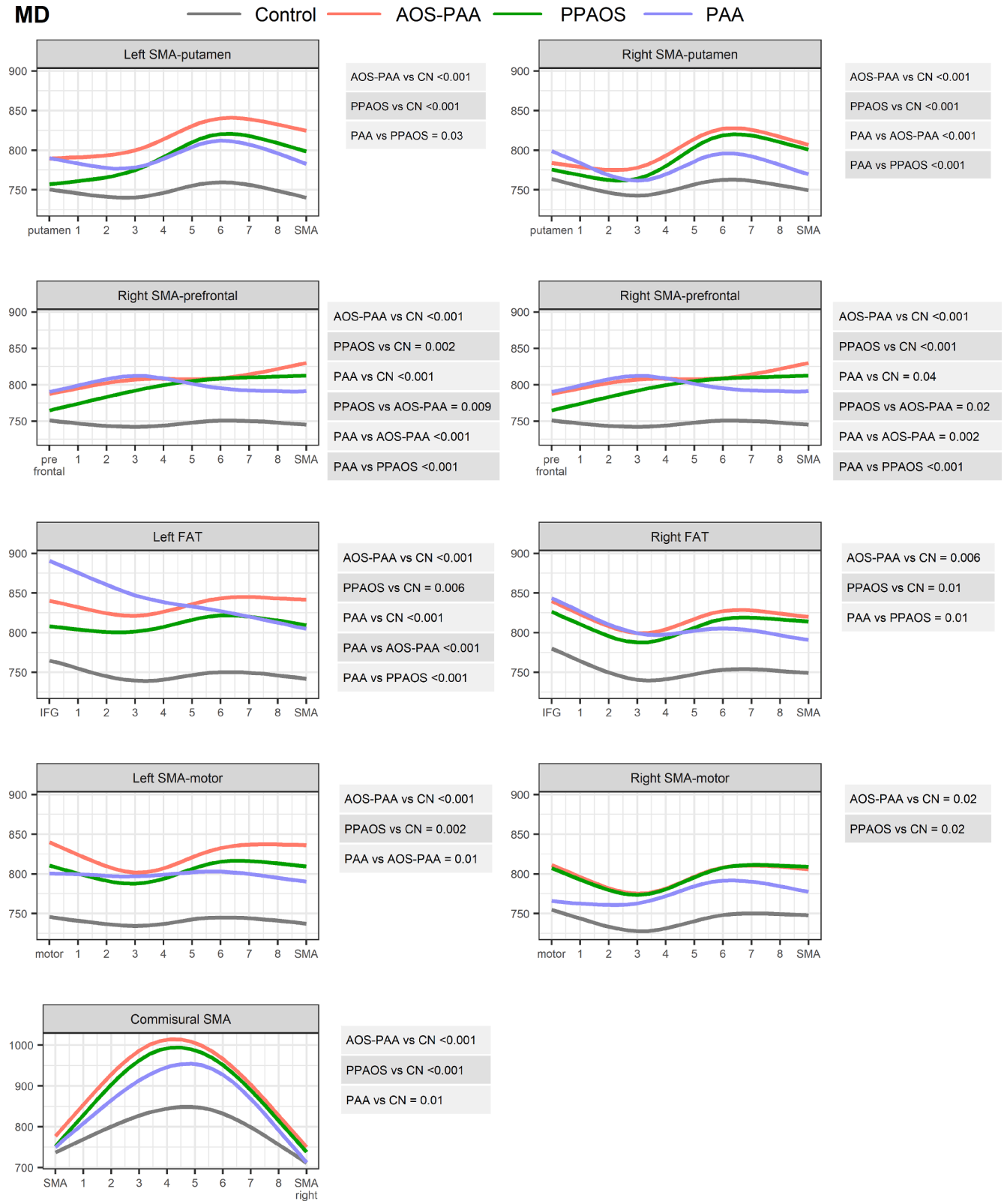

Fig. 3. Comparison of MD profiles between PPAOS, AOS-PAA, PAA and controls across tracts. Estimates from linear mixed models with restricted cubic spline fits are shown color coded for each diagnosis group for each SMA tract. P-values from a joint Wald test are shown for all significant group comparisons to the right of each plot. In the plots the first location represents the end of the tract furthest from the SMA.

Table 2

Group-wise comparisons of median values of FA, MD and number of streamlines, by tract and disease. Group-wise comparisons from Analysis of Variance, followed by Tukey Honest Significant Differences. Data shown are median (range). Median FA, MD, and # of streamlines across subjects were weighted by the number of streamlines. The MD values were multiplied by 10^6 to convert from mm^2/s to um^2/s, which makes the numbers > 1. Asymmetry scores were calculated as left hemisphere minus right hemisphere. For FA, a negative asymmetry score denotes that the left hemisphere shows more degeneration than the right. For MD, a positive asymmetry score denotes that the left hemisphere shows more degeneration than the right. Asterisks denote significantly different relative to healthy controls at *p < 0.05; **p < 0.01; ***p < 0.001. † P value compares across all four groups corrected for multiple comparisons using the false discovery rate. No significant differences were identified when comparing the three disease groups (PPAOS, AOS-PAA and PAA).

Tract	Hem	AOS-PAA	PPAOS	PAA	Control	P value†
FA						
SMA-putamen	Left	0.45 (0.41, 0.49)	0.44 (0.43, 0.46)	0.43 (0.42, 0.44)	0.47 (0.46, 0.48)	NS
	Right	0.42 (0.41, 0.47)	0.43 (0.42, 0.45)	0.43 (0.42, 0.43)	0.45 (0.44, 0.47)	NS
	L-R	0.004 (-0.008, 0.022)	0.009 (-0.005, 0.028)	0.009 (-0.005, 0.024)	0.017 (0.001, 0.026)	NS
FAT	Left	0.40 (0.38, 0.43)*	0.41 (0.39, 0.42)*	0.40 (0.39, 0.41)*	0.45 (0.43, 0.46)	0.007
	Right	0.40 (0.37, 0.44)*	0.41 (0.39, 0.43)*	0.41 (0.38, 0.42)	0.44 (0.43, 0.47)	0.02
	L-R	0.010 (-0.017, 0.018)	0.007 (-0.018, 0.023)	−0.015 (-0.030, −0.001)	0.006 (-0.013, 0.017)	NS
SMA-prefrontal	Left	0.37 (0.34, 0.40)**	0.37 (0.34, 0.39)*	0.35 (0.31, 0.37)**	0.40 (0.38, 0.43)	0.001
	Right	0.38 (0.36, 0.41)**	0.38 (0.36, 0.41)*	0.36 (0.34, 0.40)*	0.42 (0.41, 0.47)	0.002
	L-R	−0.025 (-0.037, 0.002)	−0.013 (-0.037, 0.004)	−0.032 (-0.048, −0.012)	−0.014 (-0.033, 0.003)	NS
SMA-motor	Left	0.40 (0.37, 0.41)**	0.39 (0.37, 0.41)**	0.41 (0.38, 0.41)	0.44 (0.41, 0.47)	0.003
	Right	0.41 (0.37, 0.45)	0.40 (0.38, 0.42)*	0.42 (0.39, 0.44)	0.44 (0.41, 0.47)	0.02
	L-R	−0.018 (-0.033, 0.000)	−0.012 (-0.029, 0.020)	−0.021 (-0.027, 0.001)	−0.003 (-0.013, 0.014)	NS
Commissural SMA		0.46 (0.43, 0.51)*	0.46 (0.43, 0.49)	0.49 (0.47, 0.50)	0.52 (0.50, 0.54)	0.02
MD						
SMA-putamen	Left	805 (756, 837)**	787 (757, 815)	774 (756, 812)	738 (699, 748)	0.003
	Right	781 (737, 823)	776 (725, 807)	746 (726, 775)	715 (691, 749)	0.046
	L-R	24.4 (4.0, 51.4)	14.6 (-4.0, 33.5)	29.4 (16.9, 53.0)	7.3 (0.5, 18.4)	NS
FAT	Left	824 (784, 859)**	811 (776, 835)	832 (792, 851)*	743 (705, 750)	<0.001
	Right	801 (754, 826)*	799 (748, 824)	770 (752, 822)	732 (692, 753)	0.02
	L-R	29.1 (-3.8, 54.7)	15.9 (-4.5, 32.9)	42.8 (26.0, 59.7)	1.2 (-7.7, 9.1)	NS
SMA-prefrontal	Left	820 (778, 859)**	800 (760, 833)	821 (763, 857)*	739 (707, 751)	0.002
	Right	802 (750, 829)*	788 (747, 823)	767 (754, 820)	725 (706, 744)	0.03
	L-R	23.7 (-7.0, 52.9)	10.9 (-17.8, 36.5)	29.8 (19.1, 48.8)	−5.6 (-8.6, 14.3)	NS
SMA-motor	Left	807 (773, 842)***	789 (764, 820)*	789 (764, 808)	734 (691, 743)	<0.001
	Right	775 (721, 822)*	776 (733, 810)	735 (722, 777)	718 (682, 747)	0.02
	L-R	34.5 (6.9, 74.3)	10.7 (-6.6, 43.7)	34.5 (30.1, 42.6)	3.0 (-3.3, 28.6)	0.04
Commissural SMA		877 (805, 910)**	853 (802, 895)*	805 (777, 850)	751 (712, 765)	<0.001
Number of streamlines						
SMA-putamen	Left	760 (460, 1274)	701 (490, 825)	1488 (700, 1866)	714 (427, 1222)	0.04
	Right	745 (442, 1138)	725 (503, 914)	1192 (874, 1323)	721 (543, 1135)	NS
FAT	Left	96 (58, 157)	71 (46, 121)	128 (85, 161)	37 (23, 60)	NS
	Right	108 (45, 186)	55 (23, 115)	96 (78, 119)	55 (32, 80)	NS
SMA-prefrontal	Left	208 (132, 307)	216 (133, 308)	240 (196, 282)	92 (24, 130)	NS
	Right	228 (146, 384)	192 (136, 289)	228 (172, 355)	76 (51, 188)	NS
SMA-motor	Left	204 (115, 272)	154 (103, 262)	364 (192, 488)	114 (74, 146)	NS
	Right	160 (98, 198)	117 (71, 176)	248 (111, 344)	143 (107, 204)	NS
Commissural SMA		64 (28, 110)*	44 (26, 98)	298 (132, 317)	116 (64, 206)	0.03

motor tract for MD did differ across groups, with greater left-sided asymmetry observed in AOS-PAA and PAA (Table 2). Similar trends for greater asymmetry in AOS-PAA and PAA were observed for SMA-putamen (p = 0.09), FAT (p = 0.12) and SMA-prefrontal (p = 0.14) tracts.

3.2.4. *Correlations with clinical severity*

Greater severity of AOS as measured by the ASRS was significantly associated with lower FA and greater MD in SMA commissural fibers (Spearman correlation = -0.34/p = 0.003 and 0.29/p = 0.009, respectively), as well as with greater MD in the SMA-motor tracts (Left: 0.26/p = 0.02, Right: 0.23/p = 0.04). Worse performance on the Token Test (i.e., lower score) was significantly associated with greater MD in the FAT (Left: −0.33/p = 0.006, Right: −0.25/p = 0.04) and both lower FA (Left: 0.29/p = 0.02, Right: 0.25/p = 0.04) and greater MD (Left: −0.40/p < 0.001, Right: −0.25/p = 0.04) in the SMA-prefrontal tracts.

4. Discussion

This study utilized tractography to assess differential structural connectivity of the SMA associated with progressive AOS and agrammatic aphasia. Our study design and patient groups allowed us to disentangle the effects of AOS and agrammatic aphasia by assessing patients with isolated deficits and patients that have a combination of both symptoms. We found that abnormalities in the SMA commissural fibers, SMA-putamen and SMA-motor fibers were particularly associated with AOS, while the left FAT and SMA-prefrontal fibers were particularly associated with agrammatic aphasia. Furthermore, the analysis of tract profiles showed that the tracts were most abnormal close to the SMA in PPAOS and AOS-PAA, but furthest from the SMA in those with PAA, suggesting different disease epicenters in these two syndromes.

The PPAOS group showed degeneration of all tracts from the SMA, with the most striking abnormalities observed in the SMA commissural fibers and the left SMA-motor tract. Previous structural studies have shown SMA hypometabolism and atrophy in PPAOS (Botha et al., 2015; Josephs et al., 2010; Josephs et al., 2012), with degeneration of the body of the corpus callosum observed on DTI (Josephs et al., 2012; Whitwell et al., 2013a). The striatum and motor cortex can be affected early in the disease or become affected with disease progression (Josephs et al., 2014; Tetzloff et al., 2018a; Utianski et al., 2018a). Abnormalities in PPAOS were most striking in the portions of the tracts closest to the SMA suggesting an early epicenter of degeneration in the SMA in PPAOS. Wallerian degeneration along tracts may ultimately lead to degeneration of the regions at the end of these tracts. Patients with PPAOS most commonly have an underlying 4R tau pathology (Josephs et al., 2021), and it is also possible that tract integrity is affected by progressive spread of tau from the epicenter in the SMA. Indeed, tau uptake on PET imaging is observed in the SMA in PPAOS (Utianski et al., 2018b).

Functional connectivity studies have noted a disruption between right SMA and speech and language areas in PPAOS (Botha et al., 2018). Functional MRI studies in healthy individuals also show an activation of SMA during speech tasks (Etard et al., 2000; Kawashima et al., 2000). Our findings are also in line with current models of speech production (Tourville and Guenther, 2011) in which SMA contains the initiation area for speech, gating the articulatory commands. Nevertheless, this area is not speech-specific (Basilakos et al., 2018) and may play a role in many motor and non-motor tasks controlling sequencing (Sohn and Lee, 2007), gating (Bohland et al., 2010) and motor planning (Li et al., 2016).

Our study confirms previous work which linked disruption of the FAT to language dysfunction (Catani et al., 2013). MD in the FAT correlated with aphasia severity across our cohort, particularly in the left hemisphere, and we observed abnormalities in this tract in patients with PAA. In seminal works (Catani et al., 2013) which described the role of FAT in nfvPPA the distinction between AOS and agrammatism was not made. Those studies, and some novel intraoperative language mapping reports (Dragoy et al., 2020), have related the FAT to reduced verbal fluency but not found an association with agrammatism (Catani et al., 2013). The fact that we did find a correlation between the FAT and agrammatism may reflect differences in the cohorts or the clinical measures. The FAT was abnormal in AOS-PAA which concurs with the fact that this group has agrammatic aphasia. The PPAOS group also showed involvement of the FAT, although to a lesser degree than PAA. While PPAOS patients do not have agrammatism they do show reduced speech fluency which could be related to degeneration of the FAT. However, patients with PPAOS often go on to develop agrammatic aphasia, and we have previously shown that these patients do show subtle involvement of Broca's area prior to the emergence of aphasia (Whitwell et al., 2017). Hence, involvement of the FAT in PPAOS could reflect the fact that agrammatic aphasia will develop over time in some of the cohort, although longitudinal analysis will be needed to assess this hypothesis. The fact that the PPAOS patients showed greatest abnormalities closest to the SMA fits with the explanation that spread of degeneration from the SMA to Broca's area results in the subsequent development of aphasia. In addition to the FAT, the SMA-prefrontal tract was abnormal in PAA and correlated with severity of aphasia. Damage to both the FAT and SMA-prefrontal fibers was greatest furthest from the SMA in the PAA patients, i.e., closest to Broca's area and the prefrontal ROI respectively. This is the opposite pattern to what was observed in PPAOS and suggests a disease epicenter in the inferior and middle frontal lobe in PAA with involvement of the SMA due to Wallerian degeneration or spread of pathology from the disease epicenter. Indeed, although the SMA can be atrophic in patients with PAA, the focus of neurodegeneration is the prefrontal cortex and anterior temporal lobes (Tetzloff et al., 2019).

The AOS-PAA group showed very similar patterns of tract abnormalities to PPAOS, although with greater involvement of the SMA-prefrontal tract which fits with the presence of agrammatic aphasia. There was a tendency for the FAT to show greater MD in AOS-PAA compared to PPAOS, although the difference was not significant. Patients with AOS-PAA tend to show patterns of neurodegeneration like those observed in PPAOS but with spread into the inferior frontal cortex, but with patterns very different from PAA (Josephs et al., 2013; Tetzloff et al., 2019). Hence, one could postulate that the SMA is also the epicenter of neurodegeneration in AOS-PAA but that greater involvement of the SMA tracts to the prefrontal cortex and Broca's area has resulted in the development of agrammatism.

Asymmetry was assessed in the analysis of median FA and MD across the tracts. We did not detect any differences in tract asymmetry across groups for FA, although we found some weak evidence for greater asymmetry in the AOS-PAA and PAA groups for MD, with greater MD identified in the left hemisphere in these groups. This trend was observed across all tracts but represented a significant difference for the SMA-motor tract. The tendency for left-sided asymmetry in the groups with aphasia concurs with the left-sided localization of language in these aphasic patients. We also observed stronger correlations between the FAT and Token Test in the left hemisphere. Patients with PPAOS tend to show bilateral degeneration of the SMA (Josephs et al., 2012). The lack of statistical significance in the asymmetry values could reflect variability at the patient level and reduced power due to the small sample size of the PAA group which tended to show the greatest degree of asymmetry.

Differences across the disease groups in this study were more apparent in the tract profile analysis than when assessing median metrics across the tracts, although the median FA and MD findings were consistent with the profile results when the disease groups were compared to controls. The streamline count analysis showed far fewer significant differences between the disease groups and controls. The improved sensitivity in the profile analysis may be because both FA and MD vary spatially, and the profiles provide information on *where* degeneration is happening, as opposed to the streamline count and median metrics, which are sensitive to disruption at any point along the tract. We also saw a tendency for more significant results using MD rather than FA. Tracking may be imposing a selection effect on FA since, despite the sophistication of PFT, it is difficult to propagate streamlines through low FA regions. Unlike the analysis in (Jin et al., 2017), our tract profiles are limited to detected streamlines, which is the conservative choice but neglects accounting for missing streamlines. To reduce the number of missed streamlines we used probabilistic tracking. The field of tractography has not reached a definite consensus over whether to use probabilistic or deterministic tracking (Petersen et al., 2017; Sarwar et al., 2019; Schlaier et al., 2017), but it is generally agreed that dense probabilistic tracking tends to find more connections at the risk of also producing some spurious connections, meaning that which is "better" depends on how the streamlines will be used. Many connectome studies use counts of the streamlines apparently connecting regions over the whole cortex without any a priori filtering, making false connections a major concern. Our analysis, however, filtered the streamlines in two ways (only selecting tracks passing through predefined regions, and down-weighting ones farther from the tract centroid), and was not primarily based on streamline counts, making probabilistic tracking the clear choice. Additionally, unlike MD, FA is affected by the geometry between crossing fibers, which can vary between individuals (and motivated us to use tract-based registration) but is not clearly linked to the disorders of interest to this study. We note that the uncertainty in the number of streamlines for any given tract, roughly corresponding to its volume, limits the analysis of their atrophy. We instead focus on their cellular microstructure through FA and MD. FA and MD have their limitations as microstructural probes, but more sophisticated measures are not compatible with the single b shell acquisitions that were feasible for this cohort during this period.

Strengths of our study include the large number of patients in the PPAOS and AOS-PAA groups, the fact that we had a pure AOS and a pure agrammatic group and the fact that all our patients were well characterized and diagnosed by consensus by experienced speech-language pathologists. Importantly, the strong phenotyping allowed us to make homogeneous cohorts in which comparisons could be performed and should be generalizable to other individuals with these diagnoses. The number of patients in the PAA group is, however, small which reflects how uncommon it is for patients to present with isolated agrammatism in the absence of AOS (Croot et al., 2012; Harris et al., 2013; Ogar et al., 2007; Tetzloff et al., 2019). The small sample size of the PAA group may have limited statistical power, although we still identified significant group differences despite these small samples in tracts that make biological sense for this syndrome. Additionally, because we examined multiple groups across multiple regions with different dMRI measures there is the potential for false positives. Still, our conclusions do not rest on highly localized findings that are likely to be artifacts and so we do not believe issues around multiple comparisons explain our findings. Our approach of assessing tract profiles was highly novel and sensitive. Our study design was focused only on SMA white matter tracts due to the

role of the SMA in progressive AOS. However, there may be other tracts that are important to the functional differences between these groups. The lack of a "control" tract which is unaffected in these patient groups and which could serve as a control for the method itself is also a limitation. Additionally, focusing on where the tracts are neglects where they are not, due to degeneration, although the effect of "missing" fibers is reflected in the streamline counts. Finally, care is always needed when speculating which biological processes are responsible for the changes in material properties reported by dMRI. As noted above, FA can be affected by the geometry of an individual's tract layout, in addition to processes relevant to degeneration such as demyelination and/or atrophy. MD is independent of the tract layout but can be even more sensitive than FA to the demyelination vs. atrophy degeneracy in regions where tissue loss would be filled in by CSF. The only tract in this study which directly borders CSF is the commissural SMA, which in its middle section runs along the superior surface of the ventricles. Although PFT keeps the streamlines out of the ventricles, the voxels they pass through are subject to partial volume contamination by CSF, in part due to the relatively poor spatial resolution (2.7 mm) of the diffusion voxels. The dip in FA and rise in MD in the center of the commissural SMA profiles may reflect this CSF contamination, and a thicker corpus callosum in the controls compared to the other groups. In general, the specific profiles of FA and MD that we observed in each tract likely reflect the anatomy of the tract and the tissue the tract passes through. For the FA profiles, the tracts start in a grey matter ROI and hence directional diffusion is low. FA then increases as we move to the middle of the tract and the diffusion becomes directional. In contrast, for MD, the profiles are flatter because diffusivity is more similar between grey matter and white matter, compared to the stark difference observed in FA. Tract metrics will also be affected by crossing fibers. The restricted cubic splines are not imposing a particular shape to the curves. Hence, the tract profiles are more likely to reflect underlying anatomy rather than due to limitations of our modelling technique.

The findings from this study provide insight into the breakdowns in structural connectivity that occur in patients with progressive AOS and agrammatic aphasia and suggest that these two clinical symptoms are associated with different patterns of structural breakdown in the brain. While tractography using manually placed ROIs is time consuming, automated methods could potentially provide patient-level tract data that could aid in differential diagnosis of these syndromes, particularly in differentiating PAA from PPAOS and AOS-PAA. Furthermore, understanding how the disease spreads through the brain, potentially via disrupted white matter diffusivity, will be crucial for disease modelling and for developing targeted disease biomarkers and therapies for these patients.

Funding sources

This study was funded by National Institutes of Health grants R01-DC12519, R01-DC010367, R01-DC14942 and R21-NS94684.

CRediT authorship contribution statement

Adrian Valls Carbo: Investigation, Writing – original draft. **Robert I. Reid:** Methodology, Validation, Software, Investigation, Writing – review & editing. **Nirubol Tosakulwong:** Methodology, Formal analysis, Data curation, Visualization, Writing – review & editing. **Stephen D. Weigand:** Methodology, Formal analysis, Writing – review & editing. **Joseph R. Duffy:** Investigation, Writing – review & editing. **Heather M. Clark:** Investigation, Writing – review & editing. **Rene L. Utianski:** Investigation, Writing – review & editing. **Hugo Botha:** Investigation, Writing – review & editing. **Mary M. Machulda:** Investigation, Writing – review & editing. **Edythe A. Strand:** Investigation, Writing – review & editing. **Christopher G. Schwarz:** Software, Writing – review & editing. **Clifford R. Jack:** Resources, Writing – review & editing. **Keith A. Josephs:** Investigation, Funding acquisition, Writing – review & editing. **Jennifer L. Whitwell:** Conceptualization, Supervision, Project administration, Funding acquisition, Writing – review & editing.

Declaration of Competing Interest

The authors declare that they have no known competing financial interests or personal relationships that could have appeared to influence the work reported in this paper.

References

Andersson, J.L.R., Graham, M.S., Drobnjak, I., Zhang, H., Filippini, N., Bastiani, M., 2017. Towards a comprehensive framework for movement and distortion correction of diffusion MR images: Within volume movement. Neuroimage 152, 450–466.
Andersson, J.L.R., Graham, M.S., Zsoldos, E., Sotiropoulos, S.N., 2016. Incorporating outlier detection and replacement into a non-parametric framework for movement and distortion correction of diffusion MR images. Neuroimage 141, 556–572.
Andersson, J.L.R., Sotiropoulos, S.N., 2016. An integrated approach to correction for off-resonance effects and subject movement in diffusion MR imaging. Neuroimage 125, 1063–1078.
Armstrong, M.J., Litvan, I., Lang, A.E., Bak, T.H., Bhatia, K.P., Borroni, B., Boxer, A.L., Dickson, D.W., Grossman, M., Hallett, M., Josephs, K.A., Kertesz, A., Lee, S.E., Miller, B.L., Reich, S.G., Riley, D.E., Tolosa, E., Troster, A.I., Vidailhet, M., Weiner, W.J., 2013. Criteria for the diagnosis of corticobasal degeneration. Neurology 80 (5), 496–503.
Ashburner, J., Friston, K.J., 2005. Unified segmentation. Neuroimage 26 (3), 839–851.
Avants, B.B., Tustison, N.J., Stauffer, M., Song, G., Wu, B., Gee, J.C., 2014. The Insight ToolKit image registration framework. Front Neuroinform 8, 44.
Basilakos, A., Smith, K.G., Fillmore, P., Fridriksson, J., Fedorenko, E., 2018. Functional Characterization of the Human Speech Articulation Network. Cereb. Cortex 28, 1816–1830.
Bhushan, C., Haldar, J.P., Choi, S., Joshi, A.A., Shattuck, D.W., Leahy, R.M., 2015. Co-registration and distortion correction of diffusion and anatomical images based on inverse contrast normalization. Neuroimage 115, 269–280.
Bohland, J.W., Bullock, D., Guenther, F.H., 2010. Neural representations and mechanisms for the performance of simple speech sequences. J Cogn Neurosci 22, 1504–1529.
Botha, H., Duffy, J.R., Whitwell, J.L., Strand, E.A., Machulda, M.M., Schwarz, C.G., Reid, R.I., Spychalla, A.J., Senjem, M.L., Jones, D.T., Lowe, V., Jack, C.R., Josephs, K.A., 2015. Classification and clinicoradiologic features of primary progressive aphasia (PPA) and apraxia of speech. Cortex 69, 220–236.
Botha, H., Utianski, R.L., Whitwell, J.L., Duffy, J.R., Clark, H.M., Strand, E.A., Machulda, M.M., Tosakulwong, N., Knopman, D.S., Petersen, R.C., Jack Jr., C.R., Josephs, K.A., Jones, D.T., 2018. Disrupted functional connectivity in primary progressive apraxia of speech. Neuroimage Clin 18, 617–629.
Bozkurt, B., Yagmurlu, K., Middlebrooks, E.H., Cayci, Z., Cevik, O.M., Karadag, A., Moen, S., Tanriover, N., Grande, A.W., 2017. Fiber Connections of the Supplementary Motor Area Revisited: Methodology of Fiber Dissection, DTI, and Three Dimensional Documentation. J Vis Exp.
Bozkurt, B., Yagmurlu, K., Middlebrooks, E.H., Karadag, A., Ovalioglu, T.C., Jagadeesan, B., Sandhu, G., Tanriover, N., Grande, A.W., 2016. Microsurgical and Tractographic Anatomy of the Supplementary Motor Area Complex in Humans. World Neurosurg 95, 99–107.
Catani, M., Dell'Acqua, F., Bizzi, A., Forkel, S.J., Williams, S.C., Simmons, A., Murphy, D. G., Thiebaut de Schotten, M., 2012a. Beyond cortical localization in clinico-anatomical correlation. Cortex 48 (10), 1262–1287.
Catani, M., Dell'Acqua, F., Vergani, F., Malik, F., Hodge, H., Roy, P., Valabregue, R., Thiebaut de Schotten, M., 2012b. Short frontal lobe connections of the human brain. Cortex 48 (2), 273–291.
Catani, M., Mesulam, M.M., Jakobsen, E., Malik, F., Martersteck, A., Wieneke, C., Thompson, C.K., Thiebaut de Schotten, M., Dell'Acqua, F., Weintraub, S., Rogalski, E., 2013. A novel frontal pathway underlies verbal fluency in primary progressive aphasia. Brain 136, 2619–2628.
Croot, K., Ballard, K., Leyton, C.E., Hodges, J.R., 2012. Apraxia of speech and phonological errors in the diagnosis of nonfluent/agrammatic and logopenic variants of primary progressive aphasia. J. Speech Lang. Hear. Res. 55, S1562–1572.
De renzi, E., Vignolo, L.A., 1962. The token test: A sensitive test to detect receptive disturbances in aphasics. Brain 85 (4), 665–678.
Delis, D.C., Kaplan, E., Kramer, J.H., 2001. Delis-Kaplan Executive Function System (DKEFS): Examiner's manual. The Psychological Corporation, San Antonio, TX.
Dragoy, O., Zyryanov, A., Bronov, O., Gordeyeva, E., Gronskaya, N., Kryuchkova, O., Klyuev, E., Kopachev, D., Medyanik, I., Mishnyakova, L., Pedyash, N., Pronin, I., Reutov, A., Sitnikov, A., Stupina, E., Yashin, K., Zhirnova, V., Zuev, A., 2020. Functional linguistic specificity of the left frontal aslant tract for spontaneous speech fluency: Evidence from intraoperative language mapping. Brain Lang 208, 104836.
Duffy, J.R., 2006. Apraxia of Speech in degenerative neurologic disease. Aphasiology 20 (6), 511–527.
Duffy, J.R., 2013. Motor Speech Disorders: Substrates, Differential Diagnosis and Management, 3rd ed. Elsevier, St. Louis, USA.
Etard, O., Mellet, E., Papathanassiou, D., Benali, K., Houde, O., Mazoyer, B., Tzourio-Mazoyer, N., 2000. Picture naming without Broca's and Wernicke's area. NeuroReport 11, 617–622.

Garyfallidis, E., Brett, M., Amirbekian, B., Rokem, A., van der Walt, S., Descoteaux, M., Nimmo-Smith, I., Dipy, C., 2014. Dipy, a library for the analysis of diffusion MRI data. Front. Neuroinform 8, 8.
Garyfallidis, E., Brett, M., Correia, M.M., Williams, G.B., Nimmo-Smith, I., 2012. QuickBundles, a Method for Tractography Simplification. Front. Neurosci. 6, 175.
Garyfallidis, E., Cote, M.A., Rheault, F., Sidhu, J., Hau, J., Petit, L., Fortin, D., Cunanne, S., Descoteaux, M., 2018. Recognition of white matter bundles using local and global streamline-based registration and clustering. Neuroimage 170, 283–295.
Girard, G., Whittingstall, K., Deriche, R., Descoteaux, M., 2014. Towards quantitative connectivity analysis: reducing tractography biases. Neuroimage 98, 266–278.
Goetz, C.G., Tilley, B.C., Shaftman, S.R., Stebbins, G.T., Fahn, S., Martinez-Martin, P., Poewe, W., Sampaio, C., Stern, M.B., Dodel, R., Dubois, B., Holloway, R., Jankovic, J., Kulisevsky, J., Lang, A.E., Lees, A., Leurgans, S., LeWitt, P.A., Nyenhuis, D., Olanow, C.W., Rascol, O., Schrag, A., Teresi, J.A., van Hilten, J.J., LaPelle, N., 2008. Movement Disorder Society-sponsored revision of the Unified Parkinson's Disease Rating Scale (MDS-UPDRS): scale presentation and clinimetric testing results. Movement disorders : official journal of the Movement Disorder Society 23, 2129–2170.
Gong, G., Jiang, T., Zhu, C., Zang, Y., Wang, F., Xie, S., Xiao, J., Guo, X., 2005. Asymmetry analysis of cingulum based on scale-invariant parameterization by diffusion tensor imaging. Hum. Brain Mapp. 24 (2), 92–98.
Gorno-Tempini, M.L., Hillis, A.E., Weintraub, S., Kertesz, A., Mendez, M., Cappa, S.F., Ogar, J.M., Rohrer, J.D., Black, S., Boeve, B.F., Manes, F., Dronkers, N.F., Vandenberghe, R., Rascovsky, K., Patterson, K., Miller, B.L., Knopman, D.S., Hodges, J.R., Mesulam, M.M., Grossman, M., 2011. Classification of primary progressive aphasia and its variants. Neurology 76 (11), 1006–1014.
Harris, J.M., Gall, C., Thompson, J.C., Richardson, A.M.T., Neary, D., du Plessis, D., Pal, P., Mann, D.M.A., Snowden, J.S., Jones, M., 2013. Classification and pathology of primary progressive aphasia. Neurology 81 (21), 1832–1839.
Hertrich, I., Dietrich, S., Ackermann, H., 2016. The role of the supplementary motor area for speech and language processing. Neurosci. Biobehav. Rev. 68, 602–610.
Höglinger, G.U., Respondek, G., Stamelou, M., Kurz, C., Josephs, K.A., Lang, A.E., Mollenhauer, B., Müller, U., Nilsson, C., Whitwell, J.L., Arzberger, T., Englund, E., Gelpi, E., Giese, A., Irwin, D.J., Meissner, W.G., Pantelyat, A., Rajput, A., van Swieten, J.C., Troakes, C., Antonini, A., Bhatia, K.P., Bordelon, Y., Compta, Y., Corvol, J.-C., Colosimo, C., Dickson, D.W., Dodel, R., Ferguson, L., Grossman, M., Kassubek, J., Krismer, F., Levin, J., Lorenzl, S., Morris, H.R., Nestor, P., Oertel, W.H., Poewe, W., Rabinovici, G., Rowe, J.B., Schellenberg, G.D., Seppi, K., van Eimeren, T., Wenning, G.K., Boxer, A.L., Golbe, L.I., Litvan, I., 2017. Clinical diagnosis of progressive supranuclear palsy: The movement disorder society criteria. Movement disorders : official journal of the Movement Disorder Society 32 (6), 853–864.
Jin, Y., Huang, C., Daianu, M., Zhan, L., Dennis, E.L., Reid, R.I., Jack Jr., C.R., Zhu, H., Thompson, P.M., Neuroimaging, A.D., I.,, 2017. 3D tract-specific local and global analysis of white matter integrity in Alzheimer's disease. Hum. Brain Mapp. 38, 1191–1207.
Josephs, K.A., Duffy, J.R., Clark, H.M., Utianski, R.L., Strand, E.A., Machulda, M.M., Botha, H., Martin, P.R., Pham, N.T.T., Stierwalt, J., Ali, F., Buciuc, M., Baker, M., Fernandez De Castro, C.H., Spychalla, A.J., Schwarz, C.G., Reid, R.I., Senjem, M.L., Jack Jr., C.R., Lowe, V.J., Bigio, E.H., Reichard, R.R., Polley, E.J., Ertekin-Taner, N., Rademakers, R., DeTure, M.A., Ross, O.A., Dickson, D.W., Whitwell, J.L., 2021. A molecular pathology, neurobiology, biochemical, genetic and neuroimaging study of progressive apraxia of speech. Nat. Commun. 12, 3452.
Josephs, K.A., Duffy, J.R., Fossett, T.R., Strand, E.A., Claassen, D.O., Whitwell, J.L., Peller, P.J., 2010. Fluorodeoxyglucose F18 positron emission tomography in progressive apraxia of speech and primary progressive aphasia variants. Arch. Neurol. 67, 596–605.
Josephs, K.A., Duffy, J.R., Strand, E.A., Machulda, M.M., Senjem, M.L., Gunter, J.L., Schwarz, C.G., Reid, R.I., Spychalla, A.J., Lowe, V.J., Jack Jr., C.R., Whitwell, J.L., 2014. The evolution of primary progressive apraxia of speech. Brain 137, 2783–2795.
Josephs, K.A., Duffy, J.R., Strand, E.A., Machulda, M.M., Senjem, M.L., Lowe, V.J., Jack Jr., C.R., Whitwell, J.L., 2013. Syndromes dominated by apraxia of speech show distinct characteristics from agrammatic PPA. Neurology 81, 337–345.
Josephs, K.A., Duffy, J.R., Strand, E.A., Machulda, M.M., Senjem, M.L., Master, A.V., Lowe, V.J., Jack Jr., C.R., Whitwell, J.L., 2012. Characterizing a neurodegenerative syndrome: primary progressive apraxia of speech. Brain 135, 1522–1536.
Kaufer, D.I., Cummings, J.L., Ketchel, P., Smith, V., MacMillan, A., Shelley, T., Lopez, O. L., DeKosky, S.T., 2000. Validation of the NPI-Q, a brief clinical form of the Neuropsychiatric Inventory. J. Neuropsychiatry Clin. Neurosci. 12 (2), 233–239.
Kawashima, R., Okuda, J., Umetsu, A., Sugiura, M., Inoue, K., Suzuki, K., Tabuchi, M., Tsukiura, T., Narayan, S.L., Nagasaka, T., Yanagawa, I., Fujii, T., Takahashi, S., Fukuda, H., Yamadori, A., 2000. Human cerebellum plays an important role in memory-timed finger movement: an fMRI study. J. Neurophysiol. 83 (2), 1079–1087.
Kellner, E., Dhital, B., Kiselev, V.G., Reisert, M., 2016. Gibbs-ringing artifact removal based on local subvoxel-shifts. Magn. Reson. Med. 76 (5), 1574–1581.
Kertesz, A., 2007. Western Aphasia Battery (Revised). PsychCorp, San Antonio, Tx.
Koay, C.G., Özarslan, E., Basser, P.J., 2009. A signal transformational framework for breaking the noise floor and its applications in MRI. J. Magn. Reson. 197 (2), 108–119.
Kotz, S.A., Schwartze, M., 2011. Differential input of the supplementary motor area to a dedicated temporal processing network: functional and clinical implications. Front. Integr. Neurosci. 5, 86.
Leh, S.E., Ptito, A., Chakravarty, M.M., Strafella, A.P., 2007. Fronto-striatal connections in the human brain: a probabilistic diffusion tractography study. Neurosci. Lett. 419 (2), 113–118.
Li, N., Daie, K., Svoboda, K., Druckmann, S., 2016. Robust neuronal dynamics in premotor cortex during motor planning. Nature 532 (7600), 459–464.
Luppino, G., Matelli, M., Camarda, R., Rizzolatti, G., 1993. Corticocortical connections of area F3 (SMA-proper) and area F6 (pre-SMA) in the macaque monkey. J. Comp. Neurol. 338 (1), 114–140.
Mandelli, M.L., Caverzasi, E., Binney, R.J., Henry, M.L., Lobach, I., Block, N., Amirbekian, B., Dronkers, N., Miller, B.L., Henry, R.G., Gorno-Tempini, M.L., 2014. Frontal white matter tracts sustaining speech production in primary progressive aphasia. J. Neurosci. 34 (29), 9754–9767.
Mesulam, M.-M., 1982. Slowly progressive aphasia without generalized dementia. Ann. Neurol. 11 (6), 592–598.
Mesulam, M.-M., 2001. Primary progressive aphasia. Ann. Neurol. 49 (4), 425–432.
Mita, A., Mushiake, H., Shima, K., Matsuzaka, Y., Tanji, J., 2009. Interval time coding by neurons in the presupplementary and supplementary motor areas. Nat. Neurosci. 12 (4), 502–507.
Nasreddine, Z.S., Phillips, N.A., Bedirian, V., Charbonneau, S., Whitehead, V., Collin, I., Cummings, J.L., Chertkow, H., 2005. The Montreal Cognitive Assessment, MoCA: a brief screening tool for mild cognitive impairment. J. Am. Geriatr. Soc. 53, 695–699.
Ogar, J.M., Dronkers, N.F., Brambati, S.M., Miller, B.L., Gorno-Tempini, M.L., 2007. Progressive nonfluent aphasia and its characteristic motor speech deficits. Alzheimer Dis. Assoc. Disord. 21, S23–30.
Petersen, M.V., Lund, T.E., Sunde, N., Frandsen, J., Rosendal, F., Juul, N., Ostergaard, K., 2017. Probabilistic versus deterministic tractography for delineation of the cortico-subthalamic hyperdirect pathway in patients with Parkinson disease selected for deep brain stimulation. J. Neurosurg. 126, 1657–1668.
Reid, R.I., Nedelska, Z., Schwarz, C.G., Ward, C., Jack, C.R., 2018. Diffusion Specific Segmentation: Skull Stripping with Diffusion MRI data alone. Springer, Cham.
Rey, A., 1964. L'examen clinique en psychologie. Presses Universitaires de France, Paris.
Rizzolatti, G., Luppino, G., Matelli, M., 1996. The classic supplementary motor area is formed by two independent areas. Adv. Neurol. 70, 45–56.
Sarwar, T., Ramamohanarao, K., Zalesky, A., 2019. Mapping connectomes with diffusion MRI: deterministic or probabilistic tractography? Magn. Reson. Med. 81 (2), 1368–1384.
Schlaier, J.R., Beer, A.L., Faltermeier, R., Fellner, C., Steib, K., Lange, M., Greenlee, M. W., Brawanski, A.T., Anthofer, J.M., Roeper, J., 2017. Probabilistic vs. deterministic fiber tracking and the influence of different seed regions to delineate cerebellar-thalamic fibers in deep brain stimulation. Eur. J. Neurosci. 45 (12), 1623–1633.
Schwarz, C.G., Gunter, J.L., Ward, C., Vemuri, P., Senjem, M.L., Wiste, H.J., Petersen, R. C., Knopman, D.S., Jack, C.R., 2017. The Mayo Clinic Adult Lifespan Template (MCALT): Better Quantification across the Lifespan. Alzheimer's Association International Conference.
Smith, S.M., Jenkinson, M., Johansen-Berg, H., Rueckert, D., Nichols, T.E., Mackay, C.E., Watkins, K.E., Ciccarelli, O., Cader, M.Z., Matthews, P.M., Behrens, T.E.J., 2006. Tract-based spatial statistics: voxelwise analysis of multi-subject diffusion data. Neuroimage 31 (4), 1487–1505.
Sohn, J.-W., Lee, D., 2007. Order-dependent modulation of directional signals in the supplementary and presupplementary motor areas. J. Neurosci. 27 (50), 13655–13666.
Spreen, O., Strauss, E., 1998. Compendium of Neuropsychological tests, second edition: administration, norms and commentary. Oxford University Press, New York.
Strand, E.A., Duffy, J.R., Clark, H.M., Josephs, K., 2014. The apraxia of speech rating scale: a tool for diagnosis and description of apraxia of speech. J. Commun. Disord. 51, 43–50.
Tetzloff, K.A., Duffy, J.R., Clark, H.M., Utianski, R.L., Strand, E.A., Machulda, M.M., Botha, H., Martin, P.R., Schwarz, C.G., Senjem, M.L., Reid, R.I., Gunter, J.L., Spychalla, A.J., Knopman, D.S., Petersen, R.C., Jack, C.R., Lowe, V.J., Josephs, K.A., Whitwell, J.L., 2019. Progressive agrammatic aphasia without apraxia of speech as a distinct syndrome. Brain 142, 2466-2482.
Tetzloff, K.A., Duffy, J.R., Strand, E.A., Machulda, M.M., Boland, S.M., Utianski, R.L., Botha, H., Senjem, M.L., Schwarz, C.G., Josephs, K.A., Whitwell, J.L., 2018a. Clinical and imaging progression over 10 years in a patient with primary progressive apraxia of speech and autopsy-confirmed corticobasal degeneration. Neurocase 24 (2), 111–120.
Tetzloff, K.A., Utianski, R.L., Duffy, J.R., Clark, H.M., Strand, E.A., Josephs, K.A., Whitwell, J.L., 2018b. Quantitative Analysis of Agrammatism in Agrammatic Primary Progressive Aphasia and Dominant Apraxia of Speech. J Speech Lang Hear Res 61 (9), 2337–2346.
Thompson, C.K., Ballard, K.J., Tait, M.E., Weintraub, S., Mesulam, M., 1997. Patterns of language decline in non-fluent primary progressive aphasia. Aphasiology 11 (4-5), 297–321.
Tournier, J.-D., Calamante, F., Connelly, A., 2007. Robust determination of the fibre orientation distribution in diffusion MRI: non-negativity constrained super-resolved spherical deconvolution. Neuroimage 35 (4), 1459–1472.
Tourville, J.A., Guenther, F.H., 2011. The DIVA model: A neural theory of speech acquisition and production. Lang Cogn Process 26 (7), 952–981.
Tzourio-Mazoyer, N., Landeau, B., Papathanassiou, D., Crivello, F., Etard, O., Delcroix, N., Mazoyer, B., Joliot, M., 2002. Automated anatomical labeling of activations in SPM using a macroscopic anatomical parcellation of the MNI MRI single-subject brain. Neuroimage 15 (1), 273–289.
Utianski, R.L., Duffy, J.R., Clark, H.M., Strand, E.A., Botha, H., Schwarz, C.G., Machulda, M.M., Senjem, M.L., Spychalla, A.J., Jack Jr., C.R., Petersen, R.C., Lowe, V.J., Whitwell, J.L., Josephs, K.A., 2018a. Prosodic and phonetic subtypes of primary progressive apraxia of speech. Brain Lang. 184, 54–65.

Utianski, R.L., Whitwell, J.L., Schwarz, C.G., Senjem, M.L., Tosakulwong, N., Duffy, J.R., Clark, H.M., Machulda, M.M., Petersen, R.C., Jack Jr., C.R., Lowe, V.J., Josephs, K. A., 2018b. Tau-PET imaging with [18F]AV-1451 in primary progressive apraxia of speech. Cortex 99, 358–374.

Veraart, J., Novikov, D.S., Christiaens, D., Ades-Aron, B., Sijbers, J., Fieremans, E., 2016. Denoising of diffusion MRI using random matrix theory. Neuroimage 142, 394–406.

Vergani, F., Lacerda, L., Martino, J., Attems, J., Morris, C., Mitchell, P., de Schotten, M. T., Dell'Acqua, F., 2014. White matter connections of the supplementary motor area in humans. J. Neurol. Neurosurg. Psychiatry 85 (12), 1377–1385.

Weintraub, S., Mesulam, M.-M., Wieneke, C., Rademaker, A., Rogalski, E.J., Thompson, C.K., 2009. The northwestern anagram test: measuring sentence production in primary progressive aphasia. Am J Alzheimers Dis Other Demen 24 (5), 408–416.

Whitwell, J.L., Duffy, J.R., Machulda, M.M., Clark, H.M., Strand, E.A., Senjem, M.L., Gunter, J.L., Spychalla, A.J., Petersen, R.C., Jack Jr., C.R., Josephs, K.A., 2017. Tracking the development of agrammatic aphasia: A tensor-based morphometry study. Cortex 90, 138–148.

Whitwell, J.L., Duffy, J.R., Strand, E.A., Machulda, M.M., Senjem, M.L., Gunter, J.L., Kantarci, K., Eggers, S.D., Jack Jr., C.R., Josephs, K.A., 2013a. Neuroimaging comparison of primary progressive apraxia of speech and progressive supranuclear palsy. Eur. J. Neurol. 20, 629–637.

Whitwell, J.L., Duffy, J.R., Strand, E.A., Xia, R., Mandrekar, J., Machulda, M.M., Senjem, M.L., Lowe, V.J., Jack Jr., C.R., Josephs, K.A., 2013b. Distinct regional anatomic and functional correlates of neurodegenerative apraxia of speech and aphasia: an MRI and FDG-PET study. Brain Lang. 125, 245–252.

Yeatman, J.D., Dougherty, R.F., Myall, N.J., Wandell, B.A., Feldman, H.M., 2012. Tract profiles of white matter properties: automating fiber-tract quantification. PLoS One 7, e49790.